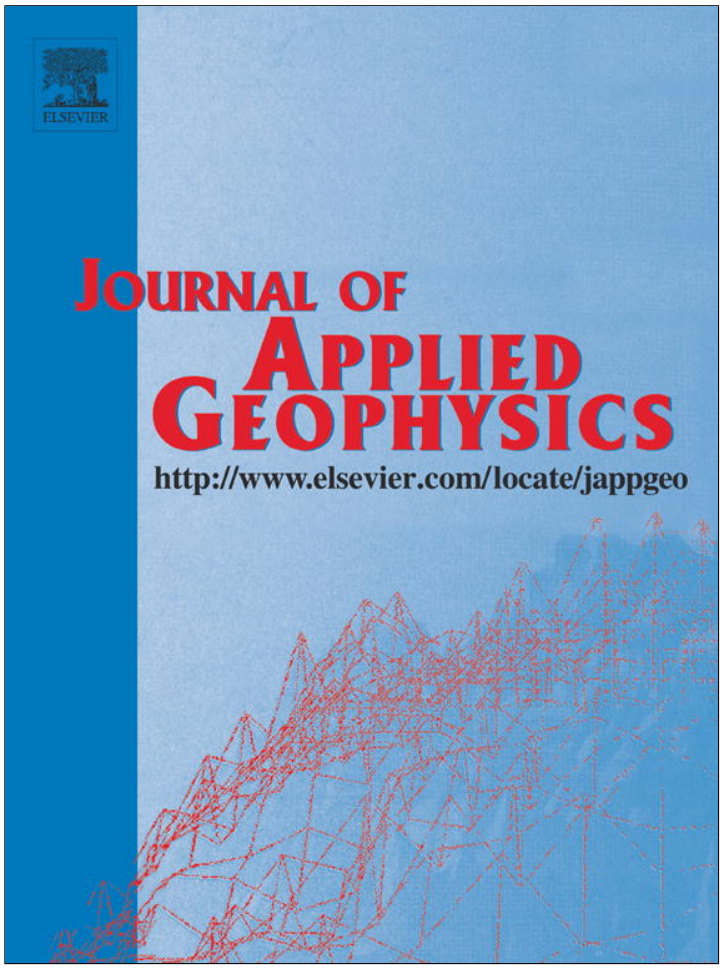

Journal of Applied Geophysics 93 (2013) 77–82

Contents lists available at SciVerse ScienceDirect

Journal of Applied Geophysics

journal homepage: www.elsevier.com/locate/jappgeo

Multiscale rock-physics templates for gas detection in carbonate reservoirs

Jing Ba [a,*], Hong Cao [a], José M. Carcione [b], Gang Tang [a], Xin-Fei Yan [a], Wei-tao Sun [c], Jian-xin Nie [d]

[a] Geophysical Department, Research Institute of Petroleum Exploration & Development, PetroChina, 100083 Beijing, China
[b] Istituto Nazionale di Oceanografia e di Geofisica Sperimentale (OGS), Borgo Grotta Gigante 42c, Sgonico, Trieste 34010, Italy
[c] Zhou Pei-Yuan Center for Applied Mathematics, Tsinghua University, 100083 Beijing, China
[d] State Key Laboratory of Explosion Science and Technology, Beijing Institute of Technology, 100081 Beijing, China

ARTICLE INFO

Article history:
Received 18 January 2013
Accepted 23 March 2013
Available online 6 April 2013

Keywords:
Rock physics model
Biot–Rayleigh theory
Heterogeneity
Porosity
Saturation
Gas reservoir identification

ABSTRACT

The heterogeneous distribution of fluids in patchy-saturated rocks generates significant velocity dispersion and attenuation of seismic waves. The mesoscopic Biot–Rayleigh theory is used to investigate the relations between wave responses and reservoir fluids. Multiscale theoretical modeling of rock physics is performed for gas/water saturated carbonate reservoirs. Comparisons with laboratory measurements, log and seismic data validate the rock physics template. Using post-stack and pre-stack seismic inversion, direct estimates of rock porosity and gas saturation of reservoirs are obtained, which are in good agreement with oil production tests of the wells.

1. Introduction

Recently, major targets of seismic exploration for oil/gas resources have been gradually shifted to highly heterogeneous reservoirs in complex geological environments. The combined analysis of multiscale wave data, which includes surface seismic data (10^{1-2} Hz), vertical seismic profile data (10^{1-3} Hz), sonic logs (10^{3-4} Hz) and laboratory measurements (10^{1-6} Hz), is useful for the detection of gas in complex heterogeneous reservoirs, since information at different spatial and frequency scales is available.

The mechanism of wave-induced local fluid flow, which is closely related to the mesoscopic heterogeneity of pore structures and fluid distributions in reservoirs, is known to induce significant velocity dispersion and attenuation of seismic waves (Ba et al., 2008a, 2011; Müller and Gurevich, 2005; Müller et al., 2010). Actually, the compressional wave velocity, which is obtained from measurements at different scales (Sams et al., 1997), is frequency-dependent as predicted by this mechanism.

Wave propagation in patchy-saturated media plays an important role in the study of multiscale wave data of gas reservoirs. Frequency-dependent P-wave velocity and attenuation can be predicted and related to the mineral and fluid properties (Dutta and Seriff, 1979; Johnson, 2001; Müller and Sahay, 2011; White, 1975). Therefore, application of the patchy-saturation theory to heterogeneous gas reservoirs has the potential of improving the use of multiscale wave data to improve the performance of hydrocarbon detection. However, mesoscopic wave theories still need further experimental validation and tests for practical applications.

Rock-physics models have been applied by Xu and White (1995), Goodway (2001) and Avseth et al. (2005) to sandstone reservoirs. Xu and Payne (2009) extended the Xu–White model, which was originally designed for clastic rocks, to carbonate rocks and their predictions are in good agreement with measurements. Generally, there are three steps in traditional rock-physics modeling: (1) Obtain the properties of grain minerals with mixing laws or effective medium theories; (2) Use of effective-medium theories, empirical relations or experimental measurements to estimate the elastic properties of the dry-rock matrix; (3) Fluid substitution. The latter is mostly treated with the Wood law and Gassmann's equations. Since the Gassmann–Wood method neglects patchy heterogeneities, a non-dispersive frequency-independent P-wave velocity is modeled. Consequently, a single rock-physics template is available at all frequencies.

In this study, the Biot–Rayleigh (BR) theory of patchy-saturated rocks (Ba et al., 2011) is used for fluid substitution. Firstly, the BR theory is compared with White's and Johnson's theories for carbonates. Regarding the in-situ petrology properties of carbonate reservoirs in Metajan district of the Right Bank Block of the Amu Darya, a multiscale rock-physics template is designed and then compared with laboratory measurements, sonic logs and surface seismic data. Based on post-stack and pre-stack inversion of surface seismic data, the template is used to estimate the porosity and gas saturation of reservoir rocks. Finally, the characteristics of the multiscale rock-physics template are summarized.

* Corresponding author. Tel.: +86 13683142802.

0926-9851/$ – see front matter © 2013 Elsevier B.V. All rights reserved.
http://dx.doi.org/10.1016/j.jappgeo.2013.03.011

2. Wave propagation theory for patchy-saturated rocks

2.1. Biot–Rayleigh theory

The double-porosity theory has been extended to describe wave propagation in patchy-saturated rocks by Pride et al. (2004), in which a branching function is used to connect the exact low- and high-frequency limits of wave dispersion and attenuation (Müller et al., 2010). Ba et al. (2011) extended the Rayleigh's (1917) formula to describe the oscillation of local fluid flow and derived dynamic equations for wave propagation in a double-porosity medium saturated with a single fluid (see Fig. 1A), which can be expressed as

$$N\nabla^2\mathbf{u}+(A+N)\nabla e+Q_1\nabla\left(\xi^{(1)}+\phi_2\varsigma\right)+Q_2\nabla\left(\xi^{(2)}-\phi_1\varsigma\right)=\rho_{11}\ddot{\mathbf{u}}+\rho_{12}\ddot{\mathbf{U}}^{(1)}+\rho_{13}\ddot{\mathbf{U}}^{(2)}+b_1\left(\dot{\mathbf{u}}-\dot{\mathbf{U}}^{(1)}\right)+b_2\left(\dot{\mathbf{u}}-\dot{\mathbf{U}}^{(2)}\right), \tag{1a}$$

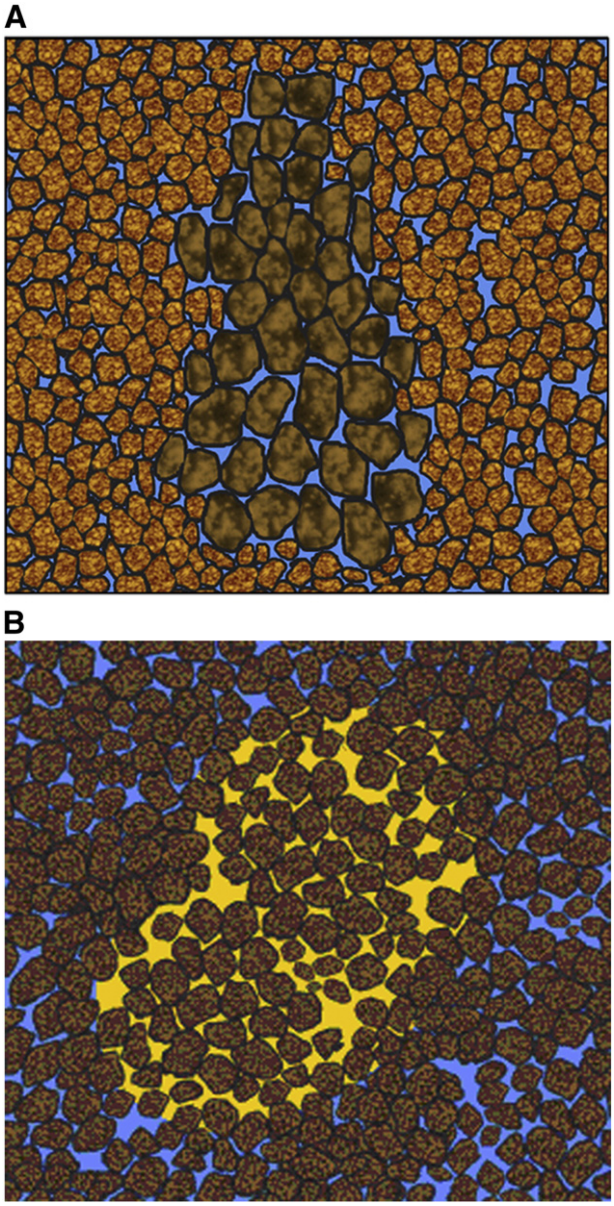

Fig. 1. Synoptic diagram for two types of mesoscopic heterogeneity in rocks. (A) A double-porosity matrix saturated with one fluid. (B) A single-porosity matrix saturated with two immiscible fluids.

$$Q_1\nabla e+R_1\nabla\left(\xi^{(1)}+\phi_2\varsigma\right)=\rho_{12}\ddot{\mathbf{u}}+\rho_{22}\ddot{\mathbf{U}}^{(1)}-b_1\left(\dot{\mathbf{u}}-\dot{\mathbf{U}}^{(1)}\right), \tag{1b}$$

$$Q_2\nabla e+R_2\nabla\left(\xi^{(2)}-\phi_1\varsigma\right)=\rho_{13}\ddot{\mathbf{u}}+\rho_{33}\ddot{\mathbf{U}}^{(2)}-b_2\left(\dot{\mathbf{u}}-\dot{\mathbf{U}}^{(2)}\right), \tag{1c}$$

$$\phi_2\left(Q_1e+R_1\left(\xi^{(1)}+\phi_2\varsigma\right)\right)-\phi_1\left(Q_2e+R_2\left(\xi^{(2)}-\phi_1\varsigma\right)\right)=\frac{1}{3}\rho_f^{(1)}\ddot{\varsigma}R_0^2\frac{\phi_1^2\phi_2\phi_{20}}{\phi_{10}}+\frac{1}{3}\frac{\eta_1\phi_1^2\phi_2\phi_{20}}{\kappa_{10}}\dot{\varsigma}R_0^2, \tag{1d}$$

where $\mathbf{u}$, $\mathbf{U}^{(1)}$ and $\mathbf{U}^{(2)}$ are the average particle displacements of the solid frame, fluid phase 1 (the fluid in the host medium) and fluid phase 2 (the fluid in the inclusions) respectively, and e, $\xi^{(1)}$ and $\xi^{(2)}$ are the corresponding displacement divergence fields of the three phases. The scalar ς represents fluid variation in local fluid flow. ϕ_{10} and ϕ_{20} are the porosities of the host medium and inclusions, respectively. ϕ_1 and ϕ_2 are the absolute porosities of the host and inclusions ($\phi_1=\nu_1\phi_{10}$ and $\phi_2=\nu_2\phi_{20}$, where ν_1 and ν_2 are the volume ratios of host medium and inclusion and $\nu_1+\nu_2=1$. $\phi=\phi_1+\phi_2$ is the porosity of the whole matrix). κ_{10} is the permeability of the host medium. η_1 and $\rho_f^{(1)}$ are the fluid viscosity and density of the host medium, respectively. R_0 is the inclusion radius. b_1 and b_2 are Biot's dissipation coefficients.

The theory has been reformulated for patchy-saturated rocks by Ba et al. (2012), where a single-porosity medium is saturated with two fluids (see Fig. 1B). In this case Eq. (1) is still available, but the host medium and inclusions have the same frame ($\phi_{10}=\phi_{20}=\phi$) and are saturated with different fluids. ϕ_1 and ϕ_2 are the relative porosities of the two types of pores which are saturated with different fluids; ν_1 (ν_2) indicates saturation and R_0 is the radius of gas pockets. The reformulated elastic constants for a patchy-saturated rock can be expressed as (Ba et al., 2012; Sun et al., submitted for publication)

$$A=(1-\phi)k_s-\frac{2}{3}N-\frac{\phi_1(1-\phi-k_b/k_s)k_s^2/k_f^{(1)}}{1-\phi-k_b/k_s+\phi k_s/k_f^{(1)}}-\frac{\phi_2(1-\phi-k_b/k_s)k_s^2/k_f^{(2)}}{1-\phi-k_b/k_s+\phi k_s/k_f^{(2)}}, \tag{2a}$$

$$Q_1=\frac{(1-\phi-k_b/k_s)\phi_1k_s}{1-\phi-k_b/k_s+\phi k_s/k_f^{(1)}}, \tag{2b}$$

$$Q_2=\frac{(1-\phi-k_b/k_s)\phi_2k_s}{1-\phi-k_b/k_s+\phi k_s/k_f^{(2)}}, \tag{2c}$$

$$R_1=\frac{\phi\phi_1k_s}{1-\phi-k_b/k_s+\phi k_s/k_f^{(1)}}, \tag{2d}$$

$$R_2=\frac{\phi\phi_2k_s}{1-\phi-k_b/k_s+\phi k_s/k_f^{(2)}}, \tag{2e}$$

$$N=\mu_b, \tag{2f}$$

where k_s, k_b, $k_f^{(1)}$ and $k_f^{(2)}$ are the bulk moduli of the solid grain, dry rock skeleton, fluid in the host medium and fluid in the inclusions, respectively; μ_b is the dry-rock shear modulus. The density coefficients are

$$(1-\phi_1-\phi_2)\rho_s=\rho_{11}+\rho_{12}+\rho_{13}, \tag{3a}$$

$$\phi_1\rho_f^{(1)}=\rho_{12}+\rho_{22}, \tag{3b}$$

$$\phi_2\rho_f^{(2)}=\rho_{13}+\rho_{33}, \tag{3c}$$

$$\rho_{22}=\alpha\phi_1\rho_f^{(1)}, \tag{3d}$$

$$\rho_{33}=\alpha\phi_2\rho_f^{(2)}, \tag{3e}$$

where ρ_s, $\rho_f^{(1)}$ and $\rho_f^{(2)}$ are the density of the three phases, and α is the tortuosity of the host medium or inclusions.

2.2. Comparisons with White's and Johnson's theories

The plane–wave solutions of Eq. (1) give three complex roots of the three types of P-waves. The velocity and attenuation of the fast P-waves are compared with laboratory measurements corresponding to Casino sandstones (Sun et al., 2012). To check the applicability of the model to partially-saturated carbonates, the experimental data reported by Cadoret et al. (1995) is compared with the BR, White and Johnson theories. The porosity and permeability of Estaillades limestone are 0.3 and 255 mD, respectively. The bulk and shear moduli of the dry-rock matrix at different frequencies are estimated from measurement. The sonic and ultrasonic P-wave velocities (KHz and 10^2 KHz) were measured with the resonant-bar and pulse-transmission techniques, respectively.

The predicted P-wave velocities by the three theories and the data corresponding to this bioclastic limestone are shown in Fig. 2. The size of the gas pocket changes with saturation, since the radius of the outer water shell (R_b, see White (1975) and Johnson (2001)) is fixed at 1.05 cm, which gives the best fit. The same radius is used for the three theories. In the sonic band, the three curves approach the Biot–Gassmann–Wood (BGW) bound. At low water saturations, the predicted P-wave velocity of White's theory, corrected by Dutta and Seriff (1979), is higher than the other two predictions and does not agree with the Biot–Gassmann theory at the full gas saturation limit. In ultrasonic band, the theoretical curves are close to the Biot–Gassmann–Hill (BGH) bound. At high water saturations, the measured ultrasonic P-wave velocity exceeds the high BGH bound, while the BR theory gives a better estimate. The three theories underestimate the P-wave velocity. The main reason may be that the theories only consider fluid patchy distribution, while neglect the heterogeneity of the solid frame (Ba et al., 2008a, 2008b).

For applications in reservoirs detecting the difference between the BR and Gassmann theories may be not so high in low porosity rocks ($\phi < 0.05$), but the latter can only give an estimate for multi-frequency waves and will not predict any dispersion.

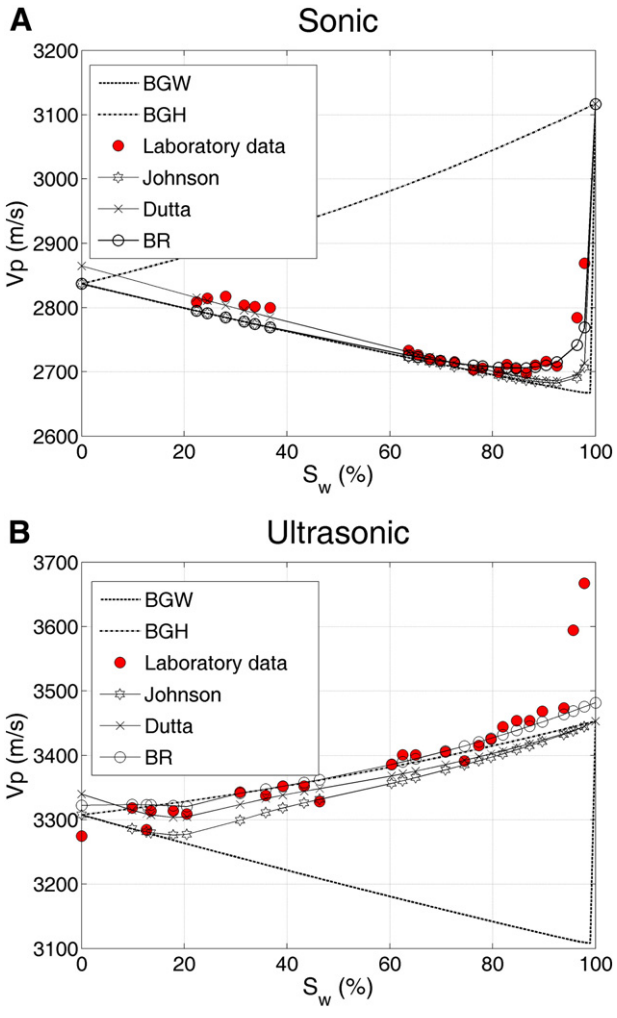

Fig. 2. Comparisons between theoretical predictions (by BR, the White's (corrected by Dutta and Seriff, 1979) and the Johnson's theories) and laboratory measurements of P-wave velocities. (A) P-wave velocity versus water saturation in the sonic frequency band (1 KHz). (B) P-wave velocity versus water saturation in the ultrasonic frequency band (500 KHz).

3. Multiscale rock-physics templates and its application

The BR theory is used for fluid substitution in this work. Firstly, we analyze the mineral components based on a geological report of the target formation. The Voigt–Reuss–Hill equation is used to calculate the elastic constants of the solid grain. The dry-rock moduli are obtained as (Pride, 2003)

$$K_b = \frac{(1-\phi)K_s}{1+c\phi}, \tag{4a}$$

$$\mu_b = \frac{(1-\phi)\mu_s}{1+c'\phi}, \tag{4b}$$

where μ_s is the shear modulus of the grains and c and c' are empirical consolidation constants (The relation between c' and c is somewhat arbitrary. Pride suggested $1.5 < c'/c < 2$ for sandstone). As mentioned above, the multiscale rock-physics template is generated with three steps: modeling the grain properties, modeling the dry-rock skeleton and fluid substitution.

Multiscale data are then compared with the templates at each scale and the coefficients are optimized, before a final seismic-band template can be generated for gas identification.

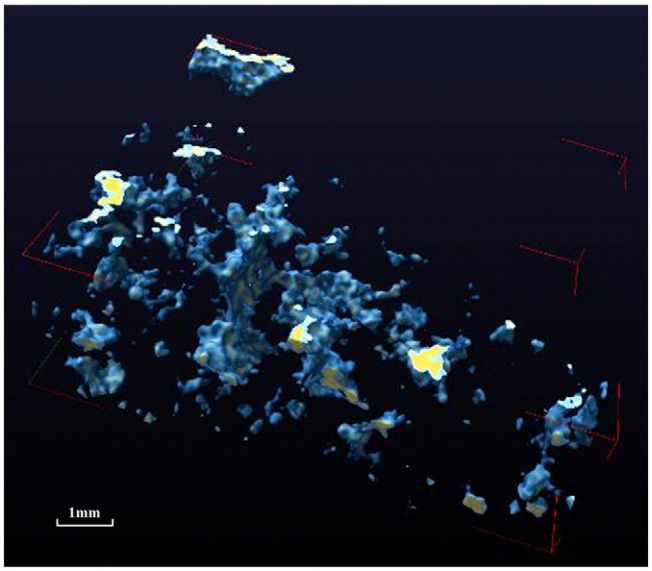

Fig. 3. Fluid distribution of a patchy-saturated oolitic limestone with a porosity of 0.16. Blue/yellow area corresponds to water/bas bearing zones, respectively. The black regions in the sample volume are the mineral grains. (For interpretation of the references to color in this figure legend, the reader is referred to the web version of this article.)

3.1. Carbonate gas reservoirs of Metajan district

Metajan district is located on the right bank of Amu Darya River, Turkmenistan. The upper Jurassic X formation is located between 2650 m and 2770 m depth, inside an open platform. Reef-flat limestone reservoirs are distributed and reservoir rocks are bioclastic limestones, oolitic limestones and gobbet limestones. The minerals are mainly calcite and clay. Dolomite is present in some regions. Rock porosity of the X formation ranges from 0.18% to 24.1%.

3.2. Multiscale rock-physics template

The size of the fluid patches in sandstone reservoir rocks is mesoscopic (Caspari et al., 2011). Our micro-CT scan study on a oolitic carbonate with a porosity of 0.16 shows very heterogeneous saturation in the millimeter scale. In Fig. 3, the yellow and blue zones indicate gas and water in pores, respectively. The size of the gas pockets is larger than the grains. The radius of gas pockets is 5 mm. We take $k_s = 76.8$ GPa, $\mu_s = 32$ GPa and $\rho_s = 2710$ kg/m^3 for the properties of the solid grain (calcite with rare clay), $k_f^{(1)} = 2.51$ GPa, $\rho_f^{(1)} = 1040$ Kg/m^3 and $\eta_1 = 0.001$ Pa s for brine and $k_f^{(2)} = 0.081$ GPa and $\rho_f^{(2)} = 170$ Kg/m^3 for the in-situ gas.

Table 1
Description of the carbonates used in this study (Adam et al., 2006; Cadoret et al., 1995).

	A	B	C	D	E	F
Porosity	0.3	0.285	0.24	0.21	0.296	0.016
Permeability	255 mD	0.43 mD	46 mD	5.5 mD	103 mD	0.03 mD
Petrography	Bioclastic limestone	–	Oolitic limestone	Dolomitic limestone	–	Dolomitic limestone

Permeability varies with porosity as $\kappa_{10} = 0.0012\ e^{63.34\phi_{10}}$. The consolidation constants c and c' are 15 and 10.5. The templates are shown in Fig. 4.

Fig. 4A shows the ultrasonic data of six carbonate samples (shown as scatters), compared with the template computed at this scale, where the wave data of A, C and G are reported from Cadoret et al. (1995) and that of B, D and E from Adam et al. (2006). The rock properties are given in Table 1. The data of A, B, C and D are in good agreement with the template. Particularly for sample A with a porosity of 0.3, the line of scatters almost coincides with the longitude line of porosity 0.3 in the template. The color variation of scatters indicates water/gas saturation and light color denotes high gas saturation, which agrees with the

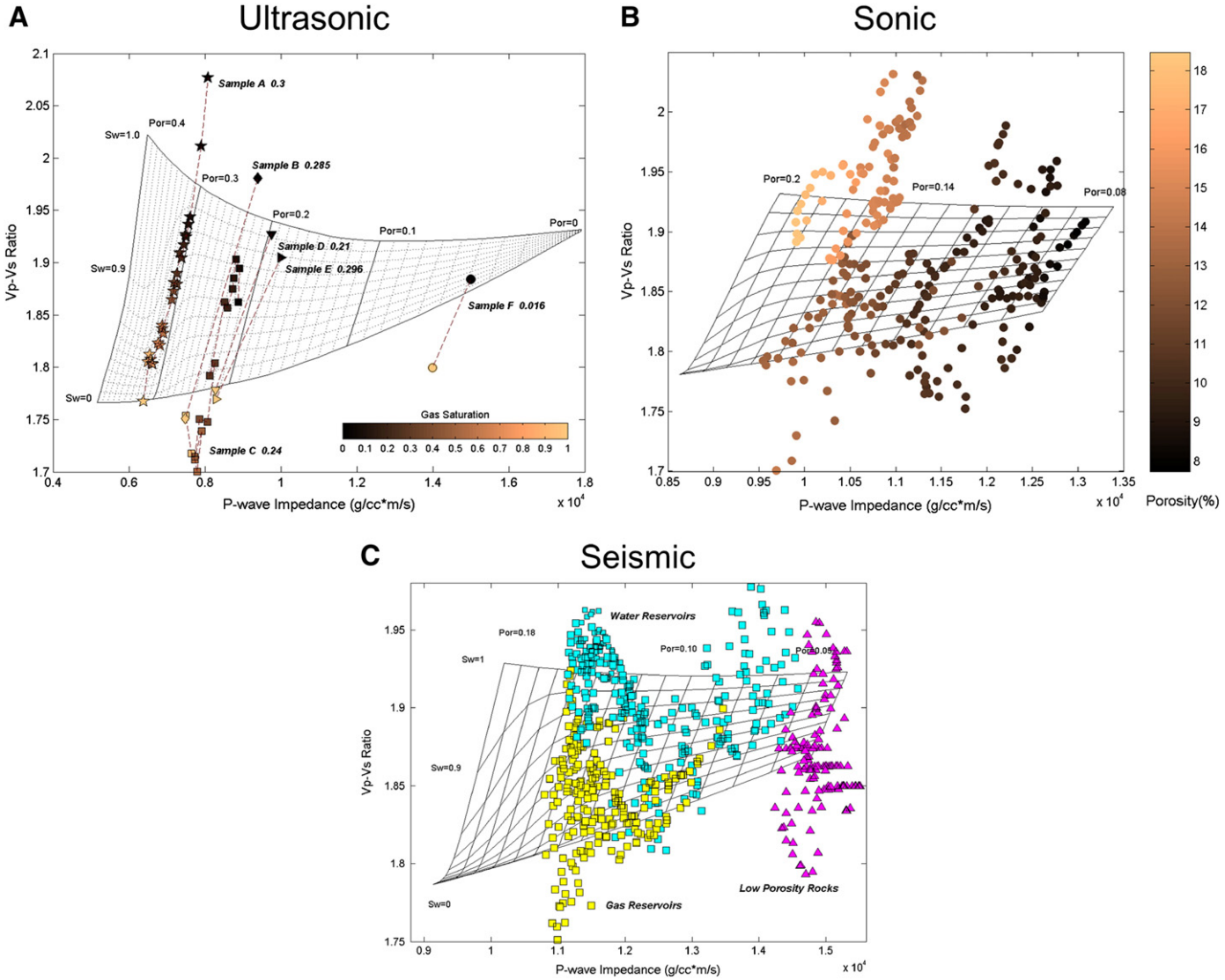

Fig. 4. Comparisons between theoretical template and measured wave data of different scales. (A) Rock physics template (ultrasonic band) and wave data from ultrasonic laboratory measurements. (B) Rock physics template (sonic band) and the fine interpretation results of sonic logs. (C) Rock physics template (seismic band) and inversion results from surface seismic data, in which low porosity rocks means "non-reservoirs" with $\phi < 5\%$. (For interpretation of the references to color in this figure, the reader is referred to the web version of this article.)

changes of latitude lines of the template. On the other hand, the template predictions disagree with the data E and F. The reason may be the heterogeneities of the grain mineral and rock frame at mesoscopic scales. Sample F is a dolomitic limestone in which micro-fractures may yield a lower P-wave velocity than that of a pure limestone with the same porosity. The petrological properties of samples A and C are close to those of the X formation, which are in good agreement with the template predictions.

Fig. 4B shows the comparison between the sonic log data (shown as scatters) and the corresponding template. The ratio of P- and S-wave velocities and P-wave impedances of the scatters are obtained from the measured interval transit time from one of the wells. The color bar indicates the interpreted porosity of reservoirs, which is in excellent agreement with the template predictions. The highest porosity of scatters is approximately 0.184, which corresponds to the actual high-porosity fully-water-saturated limestones near the X-formation bottom around this well, approaching the longitude line of porosity 0.19 and the latitude line of full water-saturation.

Fig. 4C shows the comparison between the seismic data (shown as scatters) and the corresponding template. The VP/VS ratio and P-wave impedance are extracted from the seismic traces at the borehole location after 3D post- and pre-stack inversion. The colors indicate the different kinds of rocks, which are determined through the interpretation based on seismic data and well logs. Comparing the scatters with the template shows that the porosity of gas reservoirs varies from 0.12 to 0.15 and the gas saturation varies from 30% to 100%, while the

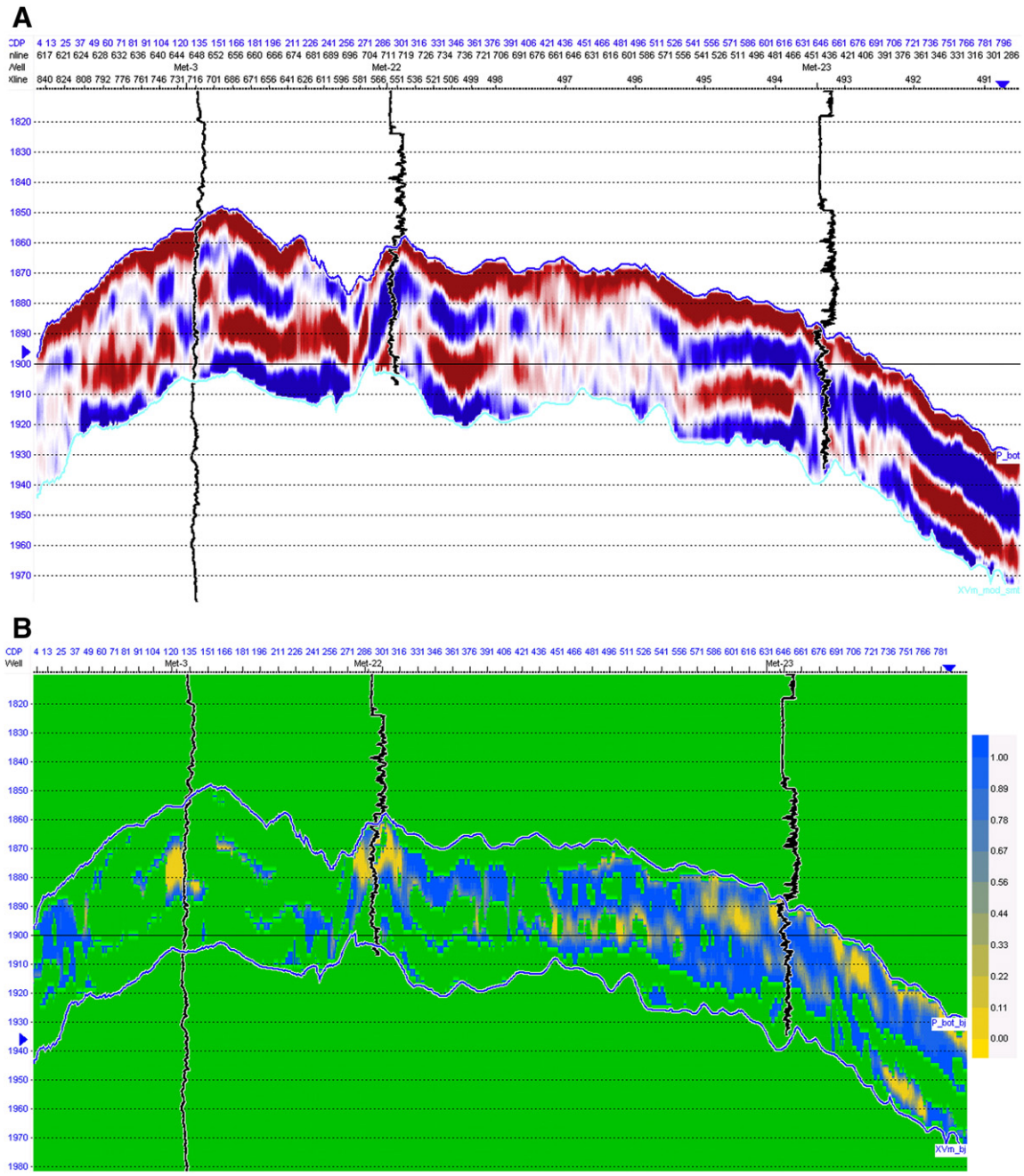

Fig. 5. 2D sections of seismic data and estimated water saturation. (A) Post-stack data of a cross-hole 2D seismic profile. (B) Section of estimated water (gas) saturation in the X formation (green for low porosity carbonate reservoirs ($\phi < 7\%$) and non-carbonates, yellow for gas reservoirs, and blue for water reservoirs). (For interpretation of the references to color in this figure legend, the reader is referred to the web version of this article.)

data corresponding to low porosity rocks lay on the right side of the porosity curve 0.05, agreeing with the geological characteristics of the X formation.

Some data points lie outside the template because they are not typical carbonate rocks which the template describes. Also, some data points lie outside due to errors in data acquisition and processing, and complexity of rock diversity, pore structures and fluid distribution. Nevertheless, the present template describes general variation trends of porosity and saturation of most of reservoir rocks.

Since the VP/VS ratio and P-wave impedance can be obtained through a pre-stack inversion, at any location of the target layer, we can overlay a point on the template with the inverted VP/VS ratio and impedance. If that point is inside the range of the template, water (gas) saturation can be estimated by finding the closest grid point.

3.3. Direct gas identification in carbonate reservoirs

Based on the analysis of the rock-physics template, the direct gas identification can be performed based on surface seismic data. Post- and pre-stack inversion is first performed on these data. The data volume of VP/VS ratio and P-wave impedance are generated and then projected onto the template at the seismic scale, and consequently the gas/water saturations in the X formation are estimated.

Fig. 5 shows the stacked data and estimated saturation of a 2D seismic profile. Three commercial gas wells (Met-3, Met-22 and Met-23) are located on this transect. Fig. 5B shows high gas-saturation areas around the wells Met-3 and Met-22, whose actual tests results of gas production of the X formation are 76.52×10^4 m^3 per day and 67.5×10^4 m^3 per day, respectively, with little water production. Fig. 5B also shows relatively lower gas saturation and high water-saturation in well Met-23, where 8.9×10^4 m^3 gas and 84 m^3 water are produced per day. The results of the direct gas identification agree with the actual test results of the three wells.

4. Conclusions

Rock-physics modeling is performed for the Metajan carbonate reservoirs. The Biot–Rayleigh theory for wave propagation in patchy-saturated rocks is used to perform fluid substitution. A frequency-dependent rock-physics template is generated and compared with the multiscale wave data. The template is applied for direct gas identification after post- and pre-stack seismic inversions. The estimated gas saturation section is in good agreement with the actual test results of gas production in the target layer. The comparisons with multiscale wave data and well test results have shown the applicability of this approach.

Multi-scale rock physics modeling is important for the oil/gas exploration industries, since more information of reservoir rocks is obtained compared to frequency-independent approaches. Furthermore, the relation between the wave responses at different frequencies (and spatial scales) can be established, which reflects the physical nature of wave dispersion and local fluid-flow mechanisms. Nevertheless, a single set of rock-physics templates is unable to fit the diversity and complexity of in-situ rocks. The possibility of non-uniqueness and misjudgment of inversion cannot be excluded in the current stage.

Other patchy-saturation theories (Johnson, 2001; White, 1975) can be similarly used in a multiscale rock physics modeling. The rock model in this paper has homogeneous solid frame while being saturated with two fluids. Solid frame heterogeneity and patchy saturation coexist in real rocks, both of which cause local fluid flow and wave dispersion. Further theoretical research should be performed for patchy-saturated rock considering a heterogeneous frame.

Acknowledgments

The authors would like to thank Beatriz Quintal, Klaus Holliger and the anonymous reviewer for their helpful comments. The authors are also grateful to Dr. David L. Johnson for providing the source code of P-wave dispersion and attenuation. This research was sponsored by NSFC (41104066, 11002025), RIPED Youth Innovation Foundation (2010-A-26-01), the 12th 5-Year Basic Research Program of CNPC (2011A-3601) and NSTMP of China (2011ZX05004-003).

References

Adam, L., Batzle, M., Brevik, I., 2006. Gassmann's fluid substitution and shear modulus variability in carbonates at laboratory seismic and ultrasonic frequencies. Geophysics 71, F13–F183.

Avseth, P., Mukerji, T., Mavko, G., 2005. Quantitative Seismic Interpretation — Applying Rock Physics Tools to Reduce Interpretation Risk. Cambridge University Press, Cambridge, UK.

Ba, J., Nie, J.X., Cao, H., Yang, H.Z., 2008a. Mesoscopic fluid flow simulation in double-porosity rocks. Geophysical Research Letters 35, L04303. http://dx.doi.org/10.1029/2007GL032429.

Ba, J., Cao, H., Yao, F.C., Nie, J.X., Yang, H.Z., 2008b. Double-porosity rock model and squirt flow in the laboratory frequency band. Applied Geophysics 5, 261–276.

Ba, J., Carcione, J.M., Nie, J.X., 2011. Biot–Rayleigh theory of wave propagation in double-porosity media. Journal of Geophysical Research 116, B06202. http://dx.doi.org/10.1029/2010JB008185.

Ba, J., Carcione, J.M., Cao, H., Du, Q.Z., Yuan, Z.Y., Lu, M.H., 2012. Velocity dispersion and attenuation of P waves in partially-saturated rocks: wave propagation equations in double-porosity medium. Chinese Journal of Geophysics 55, 219–231.

Cadoret, T., Marion, D., Zinszner, B., 1995. Influence of frequency and fluid distribution on elastic wave velocities in partially saturated limestones. Journal of Geophysical Research 100, 9789–9803.

Caspari, E., Müller, T.M., Gurevich, B., 2011. Time-lapse sonic logs reveal patchy CO_2 saturation in-situ. Geophysical Research Letters 38, L13301. http://dx.doi.org/10.1029/2011GL046959.

Dutta, N.C., Seriff, A.J., 1979. On White's model of attenuation in rocks with partial gas saturation. Geophysics 44, 1806–1812.

Goodway, B., 2001. AVO and Lamé constants for rock parameterization and fluid detection. Recorder 26, 39–60.

Johnson, D.L., 2001. Theory of frequency dependent acoustics in patchy saturated porous media. Journal of the Acoustical Society of America 110, 682–694.

Müller, T.M., Gurevich, B., 2005. Wave induced fluid flow in random porous media: attenuation and dispersion of elastic waves. Journal of the Acoustical Society of America 117, 2732–2741.

Müller, T.M., Sahay, P.N., 2011. Fast compressional wave attenuation and dispersion due to conversion scattering into slow shear waves in randomly heterogeneous porous media. Journal of the Acoustical Society of America 129 (5), 2785–2796.

Müller, T.M., Gurevich, B., Lebedev, M., 2010. Seismic wave attenuation and dispersion resulting from wave-induced flow in porous rocks—a review. Geophysics 75 (75A147-75A164).

Pride, S.R., 2003. Relationships between seismic and hydrological properties. In: Rubin, Y., Hubbard, S. (Eds.), Hydrogeophysics. Springer, pp. 253–290.

Pride, S.R., Berryman, J.G., Harris, J.M., 2004. Seismic attenuation due to wave-induced flow. Journal of Geophysical Research 109, B01201. http://dx.doi.org/10.1029/2003JB002639.

Rayleigh, L., 1917. On the pressure developed in a liquid during the collapse of a spherical cavity. Philosophical Magazine 34, 94–98.

Sams, M.S., Neep, J.P., Worthington, M.H., King, M.S., 1997. The measurement of velocity dispersion and frequency-dependent intrinsic attenuation in sedimentary rocks. Geophysics 62, 1456–1464.

Sun, W.T., Ba, J., Müller, T.M., Carcione, J.M., Cao, H., Du, Q.Z., Yan, X.F., 2012. P-wave dispersion and attenuation in patchy-saturated Rocks. White, Dutta and Biot–Rayleigh theories: the 74th EAGE in Copenhagen, Copenhagen, Denmark.

Sun, W.T., Ba, J., Ba, J., Müller, T.M., Carcione, J.M., Cao, H., 2013 Comparison of P-wave attenuation models due to wave-induced flow. Geophysical Prospecting (submitted for publication).

White, J.E., 1975. Computed seismic speeds and attenuation in rocks with partial gas saturation. Geophysics 40, 224–232.

Xu, S.Y., Payne, M.A., 2009. Modeling elastic properties in carbonate rocks. The Leading Edge 28, 66–74.

Xu, S.Y., White, R.E., 1995. A physical model for shear-wave velocity prediction. Geophysical Prospecting 44, 687–717.